

LOSSLESS COMPRESSION OF CFA-SAMPLED IMAGES USING YDGCOCG TRANSFORMS WITH CDF WAVELETS

Taizo Suzuki

Faculty of Engineering, Information and Systems, University of Tsukuba, Japan
Email: taizo@cs.tsukuba.ac.jp

ABSTRACT

This paper discusses reversible color transforms, in which a raw camera image captured using a color filter array (CFA) is from red, green, and blue (RGB) color space to YDgCoCg color space for lossless compression. We found that conventional reversible color transforms (YDgCoCg transforms) are composed of three Haar wavelets, which are simple type of wavelet. Since the finding means that the YDgCoCg transforms on the basis of other wavelets that can more accurately predict pixels of interest in the predict steps have the potential to generate more sparse signals, we replaced Haar wavelets in the YDgCoCg transforms with Cohen-Daubechies-Feauveau (CDF) 5/3 and 9/7 wavelets, which were customized on the basis of the original pixel positions in two-dimensional (2D) space. The experimental results show that the extended YDgCoCg (YDgCoCg-X) transforms, which achieve higher sparsity, outperformed the conventional transforms when they are applied to the color transform parts in the JPEG 2000 and JPEG extended range (XR) lossless modes.

Index Terms— Color filter array, lossless compression, reversible color transforms, wavelets, YDgCoCg color space.

1. INTRODUCTION

Color transforms, which change a full color image from red, green, and blue (RGB) color space to a color space expressed by one luma and two chroma components, are commonly used in image (video) preprocessing. Since more information is included in the luma component than in the chroma components, i.e., the color-transformed image is composed of sparse signals, the color transforms contribute greatly to the implementation of effective image processing, especially regarding image compression. Traditional compression standards, such as JPEG [1], JPEG 2000 [2], and MPEG-2 [3], employ the color transforms and their reversible transforms from RGB to YCbCr color space (YCbCr transforms), in which Y, Cb, and Cr are the luma, the blue-difference chroma, and the red-difference chroma components, respectively. Newer compression standards, such as JPEG extended range (XR) [4], advanced video coding (AVC) [5], and high efficiency video coding (HEVC) [6] employ the reversible color transforms from RGB to YCoCg color space (YCoCg transforms), in which Y, Co, and Cg are the luma, the orange chroma, and the green chroma components, respectively. The YCoCg transforms, which are composed of only two simple mean and difference calculations between each color component, produce more sparse signals than the YCbCr transforms.

Raw camera images captured using a color filter array (CFA), such as a Bayer pattern (shown in Fig. 1) (CFA-sampled images),

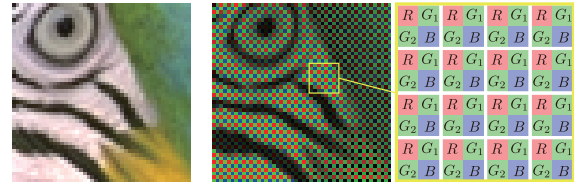


Fig. 1. Bayer pattern of a particular area of *Parrot* in Kodak images [11] (each 2×2 pixel is a macropixel): (left) full color image and (right) simulated CFA-sampled image with corresponding diagram.

are usually compressed after they are demosaiced. However, we can also choose to compress CFA-sampled images before demosaicing them because many professional photographers and designers prefer to work with them directly [7–10]. In [7], Zhang et al. discussed lossless compression of CFA-sampled images using wavelets. In [9], Lee et al. further reduced the redundancies between the chroma components generated in [7]. In [8], Malvar et al. proposed low-complexity reversible color transforms, which change a CFA-sampled image from RGB to YDgCoCg color space (YDgCoCg transforms¹) for lossless compression of CFA-sampled images. The YDgCoCg transforms are obtained by adding a different green component (Dg) to the YCoCg transforms, and they comprise of only three simple mean and difference calculations between each color component. In [10], Hernández-Cabronero et al. presented a lossless compression pipeline of CFA-sampled images, that the compressed images can be directly displayed using any JPEG 2000 standard-compliant viewer without need for additional development software, but this paper does not consider such visualization.

This paper discusses the YDgCoCg transforms for lossless compression of CFA-sampled images. We found that conventional YDgCoCg transforms are composed of three Haar wavelets, which are a simple type of wavelet. Since the finding means that the YDgCoCg transforms on the basis of other wavelets that can more accurately predict pixels of interest in the predict steps have the potential to generate more sparse signals, we replaced Haar wavelets in the YDgCoCg transforms with Cohen-Daubechies-Feauveau (CDF) 5/3 and 9/7 wavelets, which were customized on the basis of the original pixel positions in two-dimensional (2D) space. The experimental results show that the extended YDgCoCg (YDgCoCg-X) transforms, which achieve higher sparsity, outperform the conventional transforms when they are applied to the color transform parts in the JPEG 2000 and JPEG XR lossless modes.

¹This work was supported by JSPS Grant-in-Aid for Young Scientists (B), Grant Number 16K18100.

¹In [8], they are called macropixel spectral-spatial transformations (MSSTs) because they are implemented on each 2×2 macropixel.

Table 1. Coefficients of CDF 5/3 and 9/7 wavelets.

	CDF 5/3	CDF 9/7
p_0	$-1/2$	-1.586134342
u_0	$1/4$	-0.05298011854
p_1	0	0.8829110762
u_1	0	0.4435068522
s	1	1.149604398

Notation: Boldface letters represent matrices. **I**, **J**, **O**, and superscript \top indicate the 2×2 identity matrix, the 2×2 reversal matrix, the 2×2 zero matrix, and the transpose of a matrix/vector, respectively.

2. REVIEW AND DEFINITION

2.1. Cohen-Daubechies-Feauveau Wavelets

CDF wavelets are common transforms used for image processing. For practical image processing, the wavelets $\mathcal{W}(z)$ often consist of lifting schemes with predict and update steps as [12]

$$\mathcal{W}(z) = \begin{bmatrix} s & 0 \\ 0 & s^{-1} \end{bmatrix} \prod_{k=N-1}^0 \underbrace{\begin{bmatrix} 1 & U_k(z) \\ 0 & 1 \end{bmatrix}}_{\text{update step}} \underbrace{\begin{bmatrix} 1 & 0 \\ P_k(z) & 1 \end{bmatrix}}_{\text{predict step}}, \quad (1)$$

where s is a nonzero scaling coefficient, z is a delay, and $P_k(z)$ and $U_k(z)$ are lifting coefficients with arbitrary coefficients p_k and u_k as

$$P_k(z) = (1 + z^{-1})p_k \quad \text{and} \quad U_k(z) = (1 + z)u_k,$$

respectively. Furthermore, the diagonal matrix with a scaling coefficient s can be factorized into lifting schemes, such as

$$\begin{bmatrix} s & 0 \\ 0 & s^{-1} \end{bmatrix} = \begin{bmatrix} 1 & s - s^2 \\ 0 & 1 \end{bmatrix} \begin{bmatrix} 1 & 0 \\ -s^{-1} & 1 \end{bmatrix} \begin{bmatrix} 1 & s - 1 \\ 0 & 1 \end{bmatrix} \begin{bmatrix} 1 & 0 \\ 1 & 1 \end{bmatrix}. \quad (2)$$

Reversibility is achieved by applying a rounding operator to each lifting step that does not have a coefficient of $\pm i$ ($i \in \mathbb{N}$); for example, the coefficients s , p_k , and u_k in CDF 5/3 ($N = 1$) and 9/7 ($N = 2$) wavelets, as shown in Table 1. Because the CDF 5/3 and 9/7 wavelets can more accurately predict pixels of interest in the predict steps than the Haar wavelets, they generate more sparse signals.

2.2. YCoCg and YDgCoCg Transforms

The YCoCg transforms change a full color image from RGB to YCoCg color space with low-complexity calculations as (see top image in Fig. 2) [4]

$$[Y, Co, Cg]^\top = \mathbf{T} [G, R, B]^\top, \quad (3)$$

where

$$\mathbf{T} = \begin{bmatrix} 0 & 0 & 1 \\ 0 & 1 & 0 \\ 1 & 0 & 0 \end{bmatrix} \begin{bmatrix} 1 & 0 & 0 \\ 0 & 1 & 0 \\ 1/2 & 0 & 1 \end{bmatrix} \begin{bmatrix} 1 & 0 & -1 \\ 0 & 1 & 0 \\ 0 & 0 & 1 \end{bmatrix} \cdot \begin{bmatrix} 1 & 0 & 0 \\ 0 & 1 & -1 \\ 0 & 1/2 & 1 \end{bmatrix} \begin{bmatrix} 1 & 0 & 0 \\ 0 & 1 & -1 \\ 0 & 0 & 1 \end{bmatrix}. \quad (4)$$

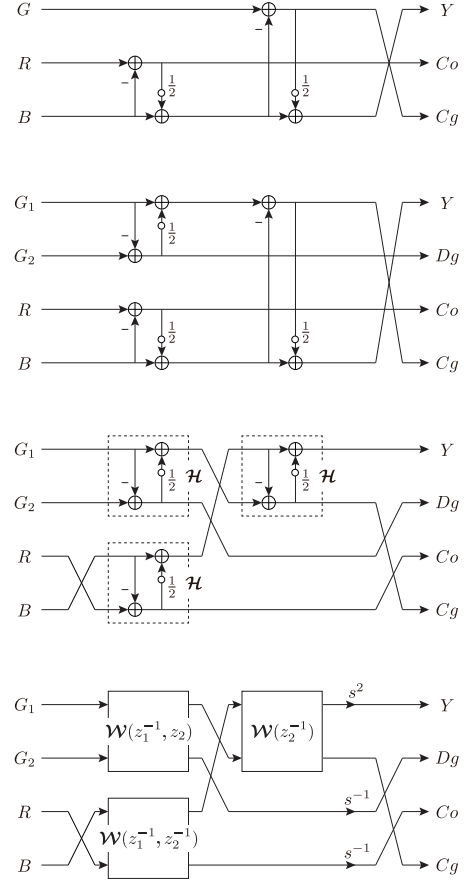


Fig. 2. Reversible color transforms (white circles represent rounding operators): (top-to-bottom) YCoCg, YDgCoCg, represented YDgCoCg, and YDgCoCg-X transforms.

Reversibility is achieved by applying a rounding operator to each lifting step that does not have a coefficient of $\pm i$.

To apply the YCoCg transforms to a CFA-sampled image, they were extended as (see the second image down in Fig. 2) [8]

$$[Y, Dg, Co, Cg]^\top = \mathcal{T} [G_1, G_2, R, B]^\top, \quad (5)$$

where

$$\mathcal{T} = \begin{bmatrix} 0 & 0 & 0 & 1 \\ 0 & 1 & 0 & 0 \\ 0 & 0 & 1 & 0 \\ 1 & 0 & 0 & 0 \end{bmatrix} \begin{bmatrix} 1 & 0 & 0 & 0 \\ 0 & 1 & 0 & 0 \\ 0 & 0 & 1 & 0 \\ 1/2 & 0 & 0 & 1 \end{bmatrix} \begin{bmatrix} 1 & 0 & 0 & -1 \\ 0 & 1 & 0 & 0 \\ 0 & 0 & 1 & 0 \\ 0 & 0 & 0 & 1 \end{bmatrix} \cdot \begin{bmatrix} 1 & 1/2 & 0 & 0 \\ 0 & 1 & 0 & 0 \\ 0 & 0 & 1 & 0 \\ 0 & 0 & 1/2 & 1 \end{bmatrix} \begin{bmatrix} 1 & 0 & 0 & 0 \\ -1 & 1 & 0 & 0 \\ 0 & 0 & 1 & -1 \\ 0 & 0 & 0 & 1 \end{bmatrix}. \quad (6)$$

The sets of R , G_1 , G_2 , and B are in macropixels, as shown in Fig. 1. Reversibility is achieved by applying a rounding operator to each lifting step that does not have a coefficient of $\pm i$. The YDgCoCg transforms \mathcal{T} are implemented as shown at the top of Fig. 3.

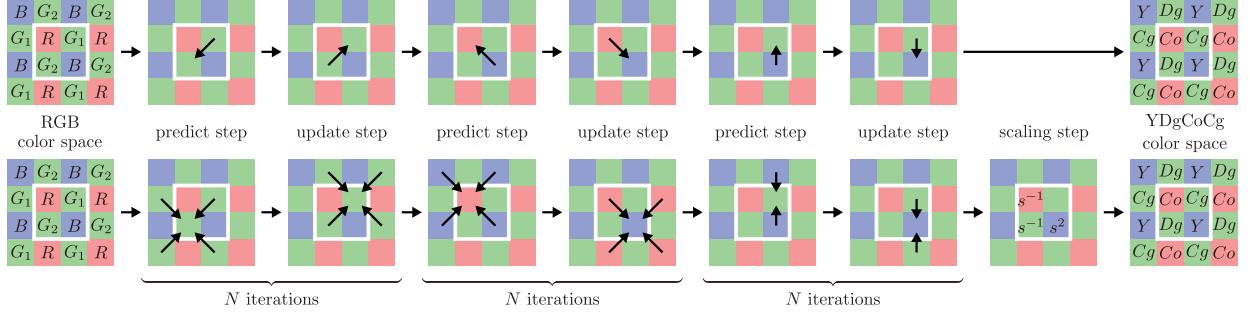


Fig. 3. Implementations: (top) the YDgCoCg transforms and (bottom) the YDgCoCg-X transforms.

3. YDGCOCG-X TRANSFORMS

Theorem: When $\mathcal{W}(z_1, z_2)$ is 2D wavelets that are customized as follows:

$$\mathcal{W}(z_1, z_2) = \prod_{k=N-1}^0 \underbrace{\begin{bmatrix} 1 & U_k(z_1, z_2) \\ 0 & 1 \end{bmatrix}}_{\text{update step}} \underbrace{\begin{bmatrix} 1 & 0 \\ P_k(z_1, z_2) & 1 \end{bmatrix}}_{\text{predict step}}, \quad (7)$$

where z_1 and z_2 are the delays horizontally and vertically, and $P_k(z_1, z_2)$ and $U_k(z_1, z_2)$ are lifting coefficients as

$$P_k(z_1, z_2) = \frac{1}{2}(1 + z_1^{-1} + z_2^{-1} + z_1^{-1}z_2^{-1})p_k$$

$$U_k(z_1, z_2) = \frac{1}{2}(1 + z_1 + z_2 + z_1z_2)u_k,$$

the YDgCoCg-X transforms \mathfrak{T} as (see the fourth image down in Fig. 2) are expressed by:

$$[Y, Dg, Co, Cg]^\top = \mathfrak{T} [G_1, G_2, R, B]^\top, \quad (8)$$

where

$$\mathfrak{T} = \underbrace{\begin{bmatrix} 1 & 0 & 0 & 0 \\ 0 & 0 & 1 & 0 \\ 0 & 0 & 0 & 1 \\ 0 & 1 & 0 & 0 \end{bmatrix}}_{\mathbf{P}_1} \begin{bmatrix} s^2 & 0 & 0 & 0 \\ 0 & 1 & 0 & 0 \\ 0 & 0 & s^{-1} & 0 \\ 0 & 0 & 0 & s^{-1} \end{bmatrix} \begin{bmatrix} \mathcal{W}(z_2^{-1}) & \mathbf{O} \\ \mathbf{O} & \mathbf{I} \end{bmatrix} \cdot \underbrace{\begin{bmatrix} 0 & 0 & 1 & 0 \\ 1 & 0 & 0 & 0 \\ 0 & 1 & 0 & 0 \\ 0 & 0 & 0 & 1 \end{bmatrix}}_{\mathbf{P}_0} \begin{bmatrix} \mathcal{W}(z_1^{-1}, z_2) & \mathbf{O} \\ \mathbf{O} & \mathcal{W}(z_1^{-1}, z_2^{-1})\mathbf{J} \end{bmatrix}. \quad (9)$$

Reversibility is achieved by applying a rounding operator to each lifting step that does not have a coefficient of $\pm i$. Note that the delay patterns in (9) are for a Bayer pattern, as shown in Fig. 1, and they depend on the original CFA pattern. The YDgCoCg-X transforms \mathfrak{T} are implemented as shown at the bottom of Fig. 3.

Proof: Haar wavelets are simple type of wavelet regarding the predict and update steps:

$$\mathcal{H} = \begin{bmatrix} 1/2 & 1/2 \\ -1 & 1 \end{bmatrix} = \underbrace{\begin{bmatrix} 1 & 1/2 \\ 0 & 1 \end{bmatrix}}_{\text{update step}} \underbrace{\begin{bmatrix} 1 & 0 \\ -1 & 1 \end{bmatrix}}_{\text{predict step}}. \quad (10)$$



Fig. 4. Test images: (top) *Akademie, Arri, Church, and Color Test Chart*, (middle) *Face, Lake Locked, Lake Pan, and Night at Odeonplatz*, (bottom) *Swimming Pool, Sharpness Chart, and Night at Siegestor*.

By using three Haar wavelets, we can represent the YDgCoCg transforms in (6) as (see the third image down in Fig. 2)

$$\mathcal{T} = \mathbf{P}_1 \begin{bmatrix} \mathcal{H} & \mathbf{O} \\ \mathbf{O} & \mathbf{I} \end{bmatrix} \mathbf{P}_0 \begin{bmatrix} \mathcal{H} & \mathbf{O} \\ \mathbf{O} & \mathcal{H}\mathbf{J} \end{bmatrix}. \quad (11)$$

To improve the transform performance, we can also use other wavelets $\mathcal{W}(z)$, such as CDF 5/3 and 9/7 wavelets, which can more accurately predict pixels of interest in the predict steps, instead of the Haar wavelets in the YDgCoCg transforms as

$$\hat{\mathfrak{T}} = \mathbf{P}_1 \begin{bmatrix} \mathcal{W}(z) & \mathbf{O} \\ \mathbf{O} & \mathbf{I} \end{bmatrix} \mathbf{P}_0 \begin{bmatrix} \mathcal{W}(z) & \mathbf{O} \\ \mathbf{O} & \mathcal{W}(z)\mathbf{J} \end{bmatrix}. \quad (12)$$

Moreover, by replacing one-dimensional (1D) wavelets $\mathcal{W}(z)$ with the 2D wavelets $\mathcal{W}(z_1^{-1}, z_2)$, $\mathcal{W}(z_1^{-1}, z_2^{-1})$, and $\mathcal{W}(z_2^{-1})$, in order to take into account the original pixel positions in 2D space, and by then merging the scaling coefficients for simplicity, we obtain the YDgCoCg-X transforms \mathfrak{T} in (9). Because the predict and update steps of the YDgCoCg-X transforms are implemented with more pixels around pixels of interest than those in the Haar wavelets, which are predicted and updated with only an adjacent pixel, the compression performance is expected to be better. Furthermore, when the YDgCoCg-X transforms \mathfrak{T} in (9) are composed of three Haar wavelets, they are equivalent to the YDgCoCg transforms \mathcal{T} in (6) and the corresponding ones in (11).

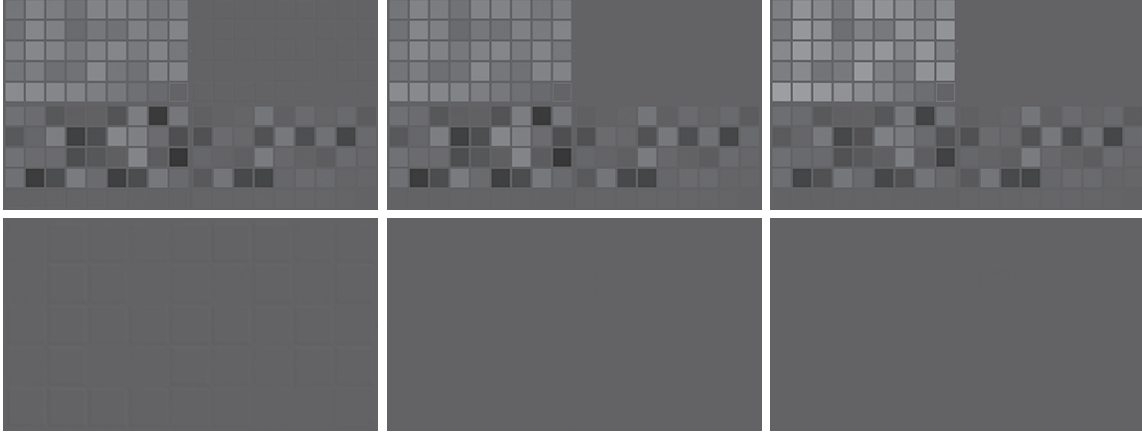


Fig. 5. Subband images of *Color Test Chart* transformed by YDgCoCg-X transforms: (top) subband images (clockwise from top-left: Y , Dg , Cg , and Co), (bottom) expanded display of the Dg components, and (left-to-right) Haar, CDF 5/3, and CDF 9/7 wavelets.

Table 2. Lossless image compression results using JPEG 2000 and JPEG XR lossless modes (lossless bitrate [bpp]).

	JPEG 2000					JPEG XR				
	[8] Haar	[9] CDF 5/3	[9] CDF 9/7	Prop. CDF 5/3	Prop. CDF 9/7	[8] Haar	[9] CDF 5/3	[9] CDF 9/7	Prop. CDF 5/3	Prop. CDF 9/7
<i>Akademie</i>	11.84	11.63	11.65	11.60	11.51	11.82	11.59	11.61	11.58	11.50
<i>Arri</i>	11.13	10.85	10.90	10.87	10.78	11.22	10.91	10.96	10.96	10.88
<i>Church</i>	10.64	10.34	10.38	10.38	10.31	10.73	10.40	10.44	10.46	10.39
<i>Color Test Chart</i>	9.82	9.94	9.98	9.73	9.71	9.84	9.94	9.97	9.76	9.74
<i>Face</i>	9.63	9.61	9.60	9.54	9.50	9.65	9.64	9.62	9.57	9.52
<i>Lake Locked</i>	10.74	10.60	10.64	10.56	10.51	10.72	10.57	10.62	10.55	10.51
<i>Lake Pan</i>	12.18	11.92	11.97	11.91	11.83	12.24	11.94	11.99	11.95	11.88
<i>Night at Odeonplatz</i>	10.51	10.54	10.57	10.41	10.39	10.49	10.52	10.54	10.40	10.37
<i>Swimming Pool</i>	11.29	11.14	11.16	11.13	11.07	11.32	11.15	11.17	11.15	11.10
<i>Sharpness Chart</i>	9.19	9.14	9.16	9.14	9.11	10.05	9.89	9.87	9.96	9.88
<i>Night at Siegestor</i>	10.48	10.49	10.51	10.37	10.35	10.45	10.45	10.47	10.34	10.33
Average	10.68	10.56	10.59	10.51	10.46	10.78	10.64	10.66	10.61	10.55

4. EXPERIMENTAL RESULTS

We compared the YDgCoCg-X transforms that used CDF 5/3 and 9/7 wavelets with the conventional transforms in [8]² and [9]³ regarding lossless bitrate [bpp] with the existing codecs, JPEG 2000 and JPEG XR, using MATLAB and Photoshop. We employed a commonly-used symmetric extension [13] at the image boundaries. As with the test images, we used 2880×1620 RGB full color images with a 16-bit dynamic range in each color component [14]. To simulate CFA-sampled images, we subsampled the test images in accordance with the Bayer pattern in Fig. 1 and reduced their dynamic range from 16 to 14-bits because the actual sensor data only had 14-bit resolution at most. Additionally, since the YDgCoCg color space has both positive and negative values, we separated the signs from the images and added them to the decoded images later. The extra 1 bit was reflected in the following results.

Figure 5 shows the subband images of the *Color Test Chart*

²The YDgCoCg transforms in [8] are equivalent with the YDgCoCg-X transforms based on Haar wavelets as previously mentioned.

³Although [7] and [9] employed “wavelet packets,” we set 1 as the wavelet level to evaluate the performance simply and fairly. Naturally, the YDgCoCg-X transforms can also use wavelet packets.

transformed by the YDgCoCg-X transforms. The YDgCoCg-X transforms that used CDF 5/3 and 9/7 wavelets reduced the redundancies between each color component compared with the YDgCoCg transforms that used Haar wavelets. Thus, the YDgCoCg-X transforms that used CDF 5/3 and 9/7 wavelets outperformed the conventional transforms when they were applied to the color transform parts in the JPEG 2000 and JPEG XR lossless modes, as shown in Table 2.

5. CONCLUSION

This paper discussed the YDgCoCg-X transforms for lossless compression of CFA-sampled images. They were obtained by replacing Haar wavelets in the YDgCoCg transforms with CDF 5/3 and 9/7 wavelets that were customized on the basis of the original pixel positions in 2D space. The experimental results showed that the proposed YDgCoCg-X transforms, which achieve higher sparsity, outperformed the conventional transforms when they were applied the color transform parts in the JPEG 2000 and JPEG XR lossless modes. Because of the high sparsity, the proposed transforms are expected to also be applied to other types of CFA-sampled image processing.

6. REFERENCES

- [1] G. K. Wallace, "The JPEG still picture compression standard," *IEEE Trans. Consum. Electr.*, vol. 38, no. 1, pp. xviii–xxxiv, Feb. 1992.
- [2] A. Skodras, C. Christopoulos, and T. Ebrahimi, "The JPEG2000 still image compression standard," *IEEE Signal Process. Mag.*, vol. 18, no. 5, pp. 36–58, Sep. 2001.
- [3] J. L. Mitchell, W. B. Pennebaker, C. Fogg, and D. J. LeGall, *MPEG Video Compression Standard*, Dordrecht, The Netherlands: Kluwer Academic, 2000.
- [4] F. Dufaux, G. J. Sullivan, and T. Ebrahimi, "The JPEG XR image coding standard," *IEEE Signal Process. Mag.*, vol. 26, no. 6, pp. 195–199, 204, Nov. 2009.
- [5] T. Wiegand, G. J. Sullivan, G. Bjøntegaard, and A. Luthra, "Overview of the H.264/AVC video coding standard," *IEEE Trans. Circuits Syst. Video Technol.*, vol. 13, no. 7, pp. 560–576, July 2003.
- [6] G. J. Sullivan, J.-R. Ohm, W.-J. Han, and T. Wiegand, "Overview of the high efficiency video coding (HEVC) standard," *IEEE Trans. Circuits Syst. Video Technol.*, vol. 22, no. 12, pp. 1649–1668, Dec. 2012.
- [7] N. Zhang and X. Wu, "Lossless compression of color mosaic images," *IEEE Trans. Image Process.*, vol. 15, no. 6, pp. 1379–1388, June 2006.
- [8] H. S. Malvar and G. J. Sullivan, "Progressive-to-lossless compression of color-filter-array images using macropixel spectral-spatial transformation," in *Proc. of DCC'12*, Snowbird, UT, Apr. 2012, pp. 3–12.
- [9] Y. Lee, K. Hirakawa, and T. Q. Nguyen, "Lossless compression of CFA sampled image using decorrelated Mallat wavelet packet decomposition," in *Proc. of ICIP'17*, Beijing, China, Sep. 2017, pp. 2721–2725.
- [10] M. Hernández-Cabronero, M. W. Marcellin, I. Blanes, and J. Serra-Sagristà, "Lossless compression of color filter array mosaic images with visualization via JPEG 2000," *IEEE Trans. Multimedia*, vol. 20, no. 2, pp. 257–270, Feb. 2018.
- [11] "Kodak Lossless True Color Image Suite," *Kodak [Online]*, Available: <http://r0k.us/graphics/kodak/>.
- [12] I. Daubechies and W. Sweldens, "Factoring wavelet transforms into lifting steps," *J. Fourier Anal. Appl.*, vol. 4, no. 3, pp. 247–269, May 1998.
- [13] M. J. T. Smith and S. L. Eddins, "Analysis/synthesis techniques for subband image coding," *IEEE Trans. Signal Process.*, vol. 38, no. 8, pp. 1446–1456, Aug. 1990.
- [14] S. Andriani, H. Brendel, T. Seybold, and J. Goldstone, "Beyond the Kodak image set: A new reference set of color image sequences," in *Proc. of ICIP'13*, Melbourne, Australia, Sep. 2013, pp. 2289–2293.